Mekanika: Majalah Ilmiah Mekanika

Seakeeping Analysis of Floating Structures with Pipe Integration Based on the Boundary Element Method

Svitlana Onyshchenko¹, Alfido Marchandi Faizatama², Nurman Firdaus^{3*}, Ristiyanto Adiputra³

- 1 Department of Fleet Operation and Shipping Technology, Odesa National Maritime University, Odesa, Ukraine
- 2 Department of Research and Development, PT. Dimonitor Indonesia Sejahtera, Surakarta, Indonesia
- 3 Research Center for Hydrodynamics Technology, National Research and Innovation Agency, Surabaya, Indonesia
- *Corresponding Author's email address: nurm006@brin.go.id

Keywords:
Hydrodynamics
Boundary element method
Cold water pipe
Mesh influence

Abstract

Floating structures are key components in offshore renewable energy systems. In the development of energy conversion, several integrated components are required, one of which is the Cold-Water Pipe (CWP). This integration will affect the interaction of the structure with environmental loads such as waves and currents, which influence the stability and seakeeping of the structure. This study employs computational analysis based on the Boundary Element Method (BEM) to more efficiently evaluate the hydrodynamic response of full-scale structures. Response Amplitude Operator (RAO), additional mass, motion response, and mooring line tension are identified as the main parameters. It was found that all these parameters are sensitive to mesh discretization. A mesh convergence study was conducted using mesh sizes of 1.8, 2.1, 2.2, and 2.3 m, which produced consistent RAO and additional mass values. Conversely, mesh sizes of 1.9, 2.0, 2.4, and 2.5 m showed inconsistencies in stability results at sea. The coarsest net (2.5 m) produced errors of up to 33% in swing, heave, and roll motions, with greater deviations in heave motion. However, tension on the mooring line remained relatively stable, indicating reduced sensitivity to variations in net size.

1 Introduction

Offshore renewable energy has become a key component in global efforts to reduce dependence on fossil fuels [1,2]. Figure 1 illustrates a comparison of energy needs by source, where the contribution of renewable energy continues to increase annually, with energy from hydro sources accounting for the most significant percentage. One rapidly developing approach to support this growth is the use of floating structures as platforms for offshore energy generation systems [3]. Floating structures require a high level of stability to withstand dynamic environmental conditions, including waves, currents, and wind. Therefore, seakeeping analysis is a crucial element in the early stages of design [4]. In practice, these structures are often integrated with additional components, such as vertical pipes that function as support system channels [5]. This integration introduces additional external forces that increase the complexity of the dynamics and affect the load distribution on the mooring system [6]. Despite the extensive research conducted on floating structures for power plants, the majority of studies remain confined to structures devoid of additional component integration [7].

https://dx.doi.org/10.20961/mekanika.v24i2.103847

Revised 25 September 2025; received in revised version 25 September 2025; Accepted 25 September 2025 Available Online 20 October 2025

2579-3144

A review of the extant literature reveals a general tendency for research to be focused on the internal analysis of vertical pipes or CWP [8], seawater tanks [9], power generation systems [10], design of vertical pipe [11], or the ultimate capacity of pipes [12]. From a hydrodynamic perspective, the integration of vertical pipes has been demonstrated to affect structural characteristics [13]. Therefore, accurately modelling the CWP in conjunction with the floating structure is imperative for capturing wave-structure interactions accurately when support components are introduced. This necessitates a meticulous approach to mesh modelling, particularly in the context of the BEM, which exhibits heightened sensitivity to surface discretization. Furthermore, the dimensions of the pipe and its connection area with the main structure have the capacity to exert influence on simulation results [14].

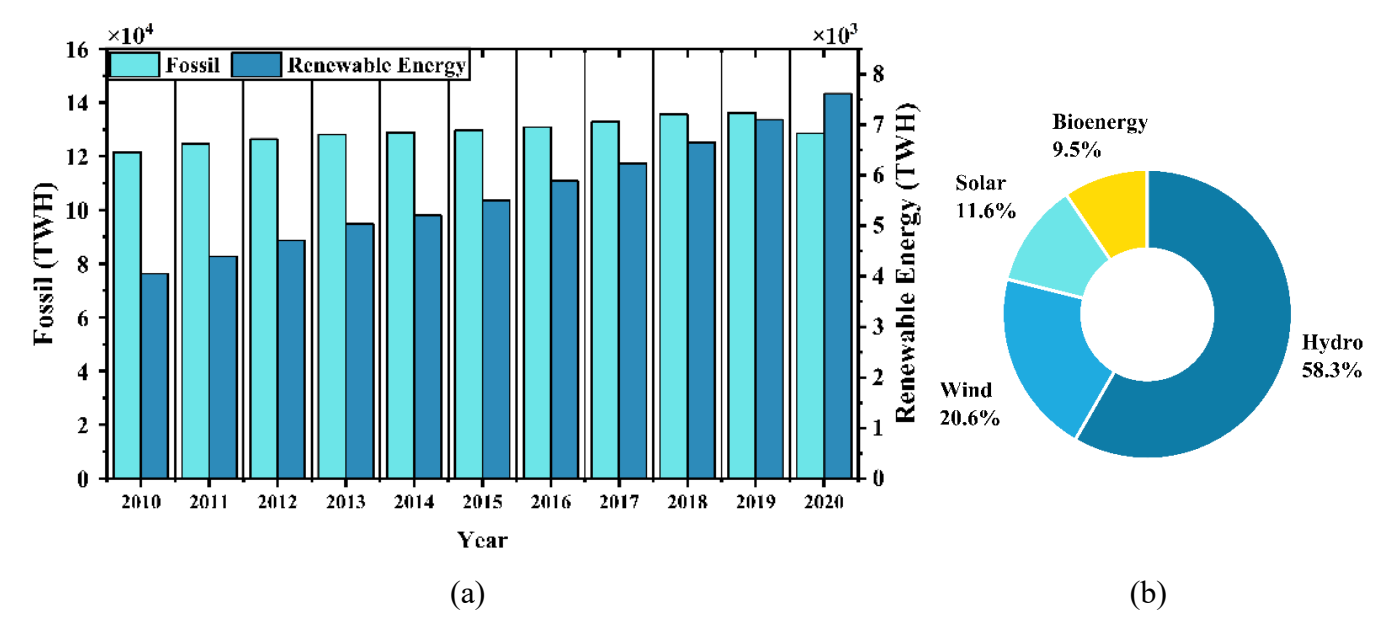


Figure 1. Comparison of growth in fossil fuel and renewable energy use (2010-2020) [1]

The present study focuses on the hydrodynamic analysis of a modified ship integrated with a CWP as part of an offshore power generation platform, incorporating a mooring system to enhance structural stability. A review of the extant literature indicates that previous studies have been limited to structural motion analysis conducted through laboratory-scale tank tests with regular and irregular waves [15]. In contrast, the present research is conducted at full scale through a series of seakeeping simulations using ANSYS AQWA based on the BEM, incorporating irregular wave and current conditions to represent realistic operational scenarios better.

The parameters analyzed include the RAO, added mass, and motion responses in both the time and frequency domains. In addition, other studies have discussed the hydrodynamic response of offshore platforms, but have not considered the sensitivity of the net or the combined evaluation of motion response and mooring line load [16]. Compared to these studies, this study expands the analysis to full-scale conditions, explicitly incorporates the effects of net discretization, and evaluates the performance of the mooring system under irregular wave-current interactions.

The novelty of this study lies in the combined application of frequency domain and time domain analyses to simultaneously evaluate motion responses and mooring line tension, thus providing a more comprehensive assessment of structural stability. Furthermore, this research explicitly investigates mesh sensitivity in BEM-based simulations for integrated CWP-ship systems, an aspect that has been rarely addressed in previous numerical or experimental works. This integrated, full-scale approach offers the advantage of delivering more realistic and accurate predictions of hydrodynamic performance and mooring loads when compared to conventional laboratory-scale or single-parameter studies.

2 Methodology

2.1 Hydrodynamic characteristics

In hydrodynamic analysis, the interaction between floating structures and waves in an infinite domain can be solved numerically using partial differential equations [17]. One commonly used approach is the BEM, which utilizes Green's theorem to transform partial differential equations into integral form on boundary surfaces. This transformation aims to simplify the calculation of hydrodynamic forces by reducing the dimension of the problem through a discretization process on the boundary surface of the structure [18]. The result of the discretization process is a system of linear equations that can be solved more efficiently numerically within the context of the BEM method. In the analysis of floating structures, several boundary conditions must be assumed, as illustrated in Figure 2.

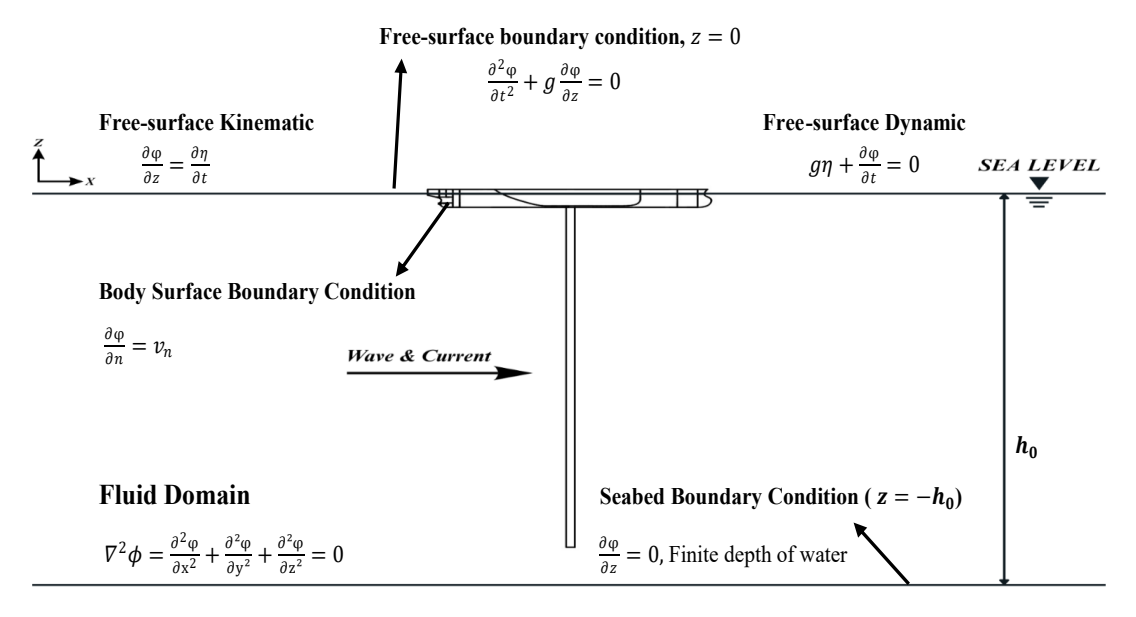


Figure 2. Boundary condition

After the implementation of the boundary conditions, an analysis of the interaction between the waves and the floating structure is conducted through a combination of the total velocity potential, which consists of three primary components: incident potential, diffraction potential, and radiation potential [19]. To facilitate numerical computations, the surface of the structure is discretized into a series of small panels, a process referred to as meshing. This approach enables the calculation of wave-structure interactions to be performed locally on each panel, thereby enhancing the accuracy of the simulation results. In this method, a Green's function is used to solve the wave equation in the fluid surrounding the structure [20]. The function under consideration herein represents the system's response to the disturbance source, describes the wave behavior in the fluid boundary condition, and takes into account the assumption of infinite water depth. Among the various methodologies proposed, seakeeping analysis can be performed by developing the fundamental equation of motion for the structure, as shown in Equation 1. To obtain the RAO and added mass values, the equation is then transformed into the frequency domain, as shown in Equation 2.

$$(M + M_a)\ddot{\xi} + B\dot{\xi} + K\xi = F \tag{1}$$

$$[-\omega^2(M+M_a)+i\omega B+K]\xi(\omega) = F_e(\omega)$$
 (2)

Where, M signifies the mass of the structure, M_a denotes the added mass, B denotes the radiation damping, K represents the restoring force, $\ddot{\xi}$ represent acceleration, $\dot{\xi}$ is velocity, ξ represent vector displacement, and $F_e(\omega)$ denotes the excitation force. The radiation damping coefficient is obtained using the potential flow theory approach. This approach involves integrating the hydrodynamic pressure related to the wave effect, as expressed by the steady-state Bernoulli equation.

2.2 Case configuration

The research methodology is summarized in the flowchart as shown in Figure 3, which outlines the sequential stages of the seakeeping analysis for the integrated structure. The process is initiated with the geometry modelling of the ship with the CWP system. This is followed by the hydrodynamic diffraction setup, in which structural parameters, such as mass definition, moment of inertia, and added mass, as well as the stiffness matrix, are determined, along with the mesh configuration. The frequency domain simulation stage involves solving the hydrodynamic diffraction problem to obtain added mass and RAO values. Subsequently, time domain simulations are performed, commencing with the design of mooring systems and the delineation of environmental conditions. The utilization of these simulation results in generating hydrodynamic response solutions, encompassing ship motions and mooring line tensions.

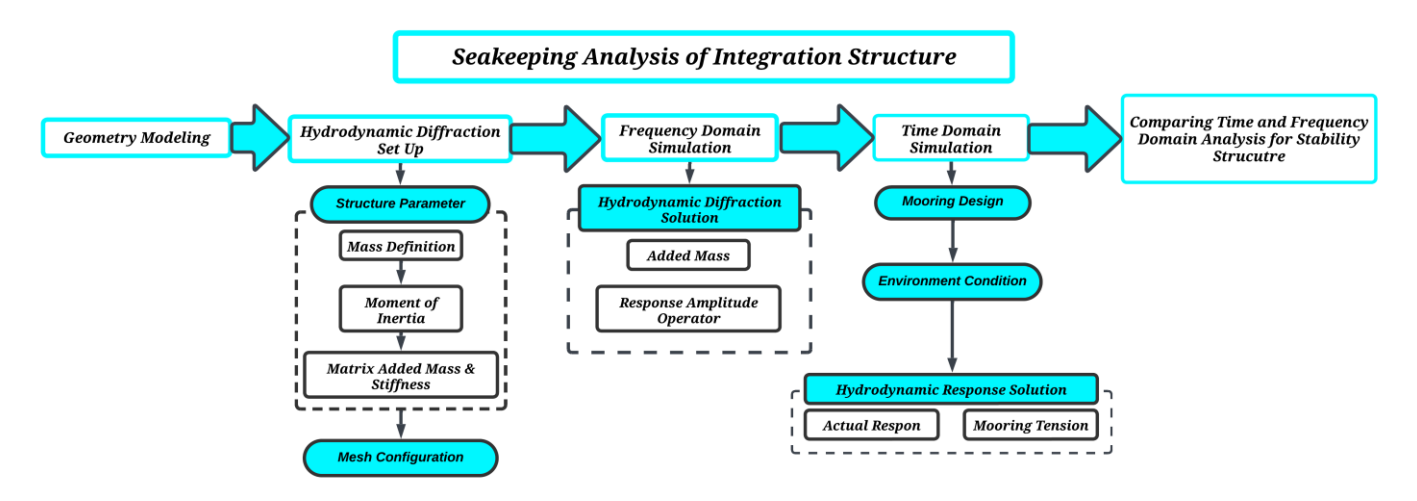


Figure 3. Research flowchart

To implement the methodology as mentioned earlier, the floating structure under consideration in this study is a ship-type configuration, with dimensions listed in Table 1. The structure is integrated with a vertical pipe that has a length of 500 meters, an outer diameter of 9.6 meters, and a wall thickness of 16 cm. The pipe is modeled as a rigid structure so that deformation or deflection due to load is ignored, as this study focuses on the seakeeping analysis of the platform as a whole. An illustration of the integration between the floating structure and the pipe is shown in Figure 4a. To ensure simulation precision, an investigative approach involving various mesh size variations was implemented on a floating structure integrated with a 500 m-long vertical pipe. The selection of this pipe length was based on a previous study that demonstrated a significant difference in response compared to other length variations [21]. Furthermore, mesh variations are employed to assess the impact of element size on hydrodynamic parameters in the time domain.

This includes the actual response of the structure and tension in the mooring system. The mesh sizes used are as follows: 1.8, 1.9, 2.0, 2.1, 2.2, 2.3, 2.4, and 2.5 m. To maintain position stability and limit unwanted horizontal movement, primarily due to long-term drift forces, the floating structure is equipped with a mooring system. A schematic of the mooring system is shown in Figure 4b, where the mooring system consists of four mooring lines, each with a length of 4000 meters, divided into two segments: a 1500-meter chain segment and a 2500-meter wire segment. The chain segment uses type Q5 with a diameter of 0.12 meters, a maximum expected tension of 15.8 MN, a stiffness of 2.13 GN, and a linear mass of 263.4 kg/m [22]. Meanwhile, the wire segment has an equivalent diameter of 0.232 meters, a maximum expected tension of 15.7 MN, a stiffness of 0.429 GN, and a linear mass of 75 kg/m. This mooring system configuration is designed to effectively resist environmental loads such as waves, currents, and wind, and to ensure the stability and safety of the structure during operations in the open sea. Following the modeling of the mooring system, environmental conditions were modeled based on Korea Research Institute of Ships and Ocean Engineering (KRISO) Ocean Basin data, which have been utilized in previous studies.

The waves were modeled as irregular waves with a Joint North Sea Wave Project (JONSWAP) spectrum, using a significant wave height of 2.48 m and a peak period of 9.87 s. In addition, an ocean current of 1.4 m/s was added [23]. The incident wave and current directions were set at 90°, which is representative of beam sea conditions.

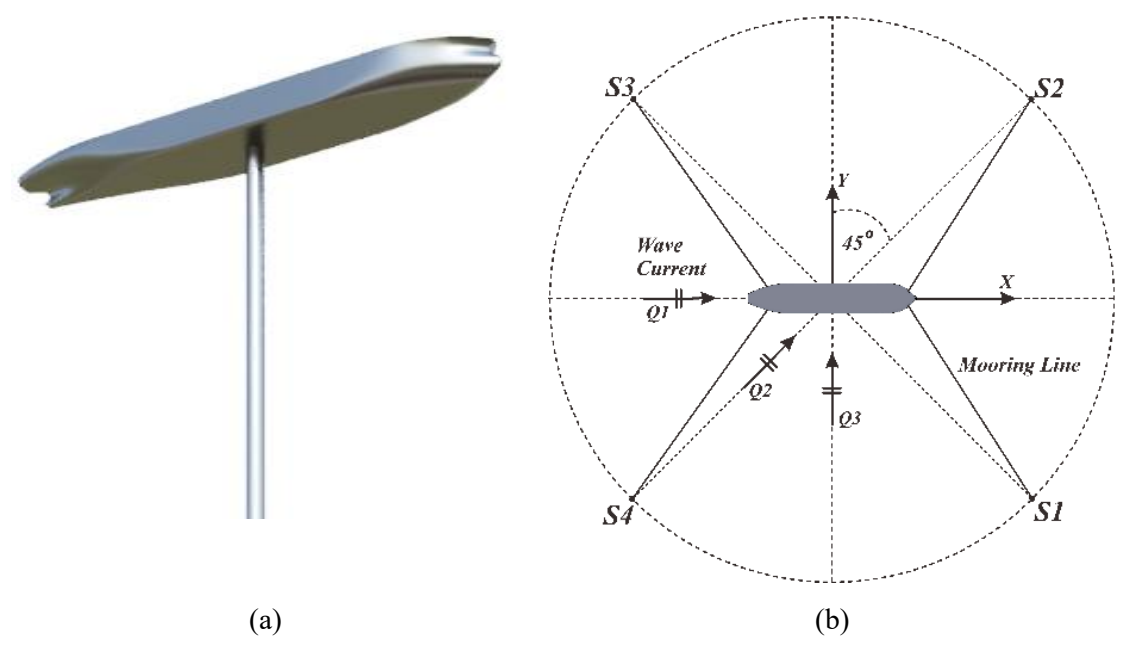


Figure 4. Integration structure: (a) Floater and pipe and (b) Floater and mooring

Table 1	I. Floating	structure	dimension	[15	

Parameters	Unit	Value
length between perpendicular	m	300
breadth	m	54.6
height	m	24.6
draft	m	19.5
vertical center of gravity	m	-3.6
radius of gyration (R_{XX}, R_{YY}, R_{ZZ})	m	(19, 75, 78)

3 Result and Discussion

3.1 Added mass

The results of the mesh size sensitivity analysis of the heave and roll added mass values of the floating structure integrated with the vertical pipe are shown in Figure 5. For the purpose of analyzing heave motion, the value of added mass is observed to decrease until it reaches approximately 2.5×10^8 kg at a frequency of 0.5 rad/s. Thereafter, an increase in the value of added mass is noted as the frequency increases. A general observation indicates that all mesh variations demonstrate analogous and consistent trends. This finding suggests that the interaction of fluid mass with heave motion is predominantly significant at low frequencies, while at high frequencies, the value remains relatively constant. However, at frequencies ranging from 0.7 to 0.8 rad/s, the 1.9 m mesh displays a substantial decline, resulting in negative added mass values. In contrast, the 2 m mesh exhibits a pronounced surge. This finding suggests numerical instability resulting from inadequate mesh size or ineffective panel distribution within critical regions [24]. Conversely, the 2.1 to 2.5 m mesh generates smooth and stable curves, rendering it more suitable for hydrodynamic simulations, where it accurately represents the surface conditions of the structure. In roll motion, a substantial discrepancy in the value of added mass emerges between mesh size variations. The maximum value is observed at a mesh size of 2 m, which yields approximately 1.85×10^{11} kg.m²/deg. Conversely, other mesh variations demonstrate a lesser disparity and exhibit a trend that remains consistent with frequency.

This phenomenon suggests a correlation between the discrepancy in roll-added mass and the precision of the mesh utilized [24]. As the mesh size increases, the detailed geometry and pressure distribution on the surface of the structure are not optimally represented, resulting in more conservative calculations. It has been demonstrated that larger panels are incapable of capturing the complexity of wave interaction with the structure, especially in areas with high pressure gradients.

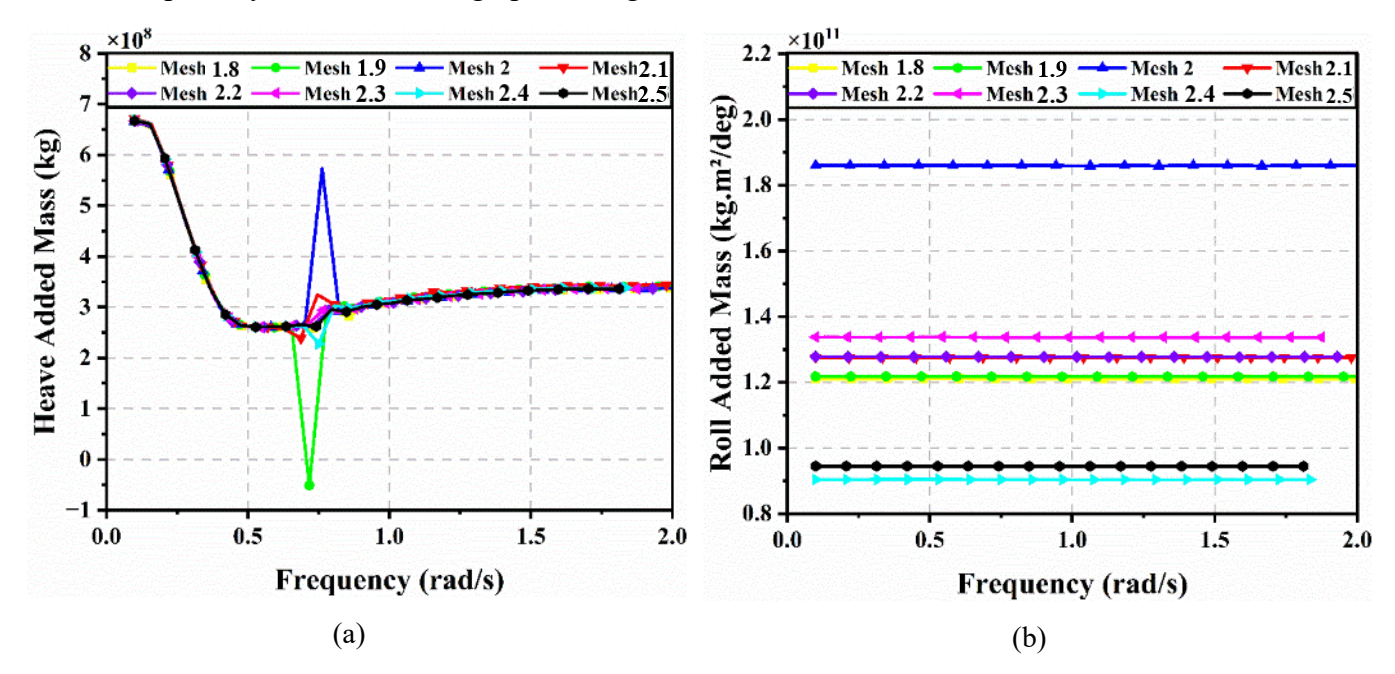


Figure 5. Added mass of floating structure in: (a) Heave and (b) Roll

3.2 Response amplitude operator

In the analysis of the stability of floating structures, the RAO is utilized to predict the response of structures to linear sea waves based on wave frequency and amplitude. Before the primary analysis, a comparison test was conducted for a ship without CWP and for a ship integrated with a 240 m CWP in numerical studies and experiments, which was the configuration used in the pioneering research. The errors observed were approximately 5% for heave and roll movements, and 12% for pitch movements [15]. These were deemed to be acceptable for validation against experimental parameters [25]. These RAO values form the basis for evaluating the dynamic performance of the structure and developing a more effective design. Figure 6 presents the results of RAO analysis for heave, roll, and pitch motions for different mesh size variations. The heave motion exhibits consistency in amplitude across mesh variations, with the peak value occurring at a frequency of approximately 0.5 rad/s and an amplitude of approximately 1.3 m/m. This stability reflects that the potential distribution of fluid flow around the structure in the vertical direction is more evenly distributed, resulting in more accurate hydrodynamic calculations that are not sensitive to variations in mesh panel size. For roll motion, there is little difference in response between mesh variations.

At mesh sizes of 1.9, 2.0, and 2.5 m, the peak RAO values are slightly lower than the other variations and occur at frequencies that are slightly shifted from the principal resonance value (around 0.23 rad/s with a maximum amplitude of 0.42 deg/m). This difference indicates that the panels at this mesh size are less capable of optimally representing the surface of the structure, especially in areas with high pressure gradients due to wave moments, resulting in inaccurate predictions of the resonance response. Regarding the pitch motion, the RAO results reveal more significant amplitude variations between mesh sizes. Especially in the 2.0, 2.4, and 2.5 m meshes, there is a considerable difference in amplitude. This indicates that in longitudinal rotational motions, the sensitivity to the size and distribution of mesh panels is higher due to differences in pressure distribution that are not accurately calculated, particularly when mesh sizes are too coarse or less adaptive to the structure's contours.

In general, the results of RAO analysis in all three modes of motion indicate that the selection of mesh size has a significant impact on the accuracy of the simulation results. Mesh size variations, such as 1.8, 2.1, 2.2, and 2.3 m, demonstrate consistency and stability of results across all analyzed modes of motion. This confirms the importance of selecting and distributing mesh elements properly in hydrodynamic simulations to obtain representative results that are free from numerical instability.

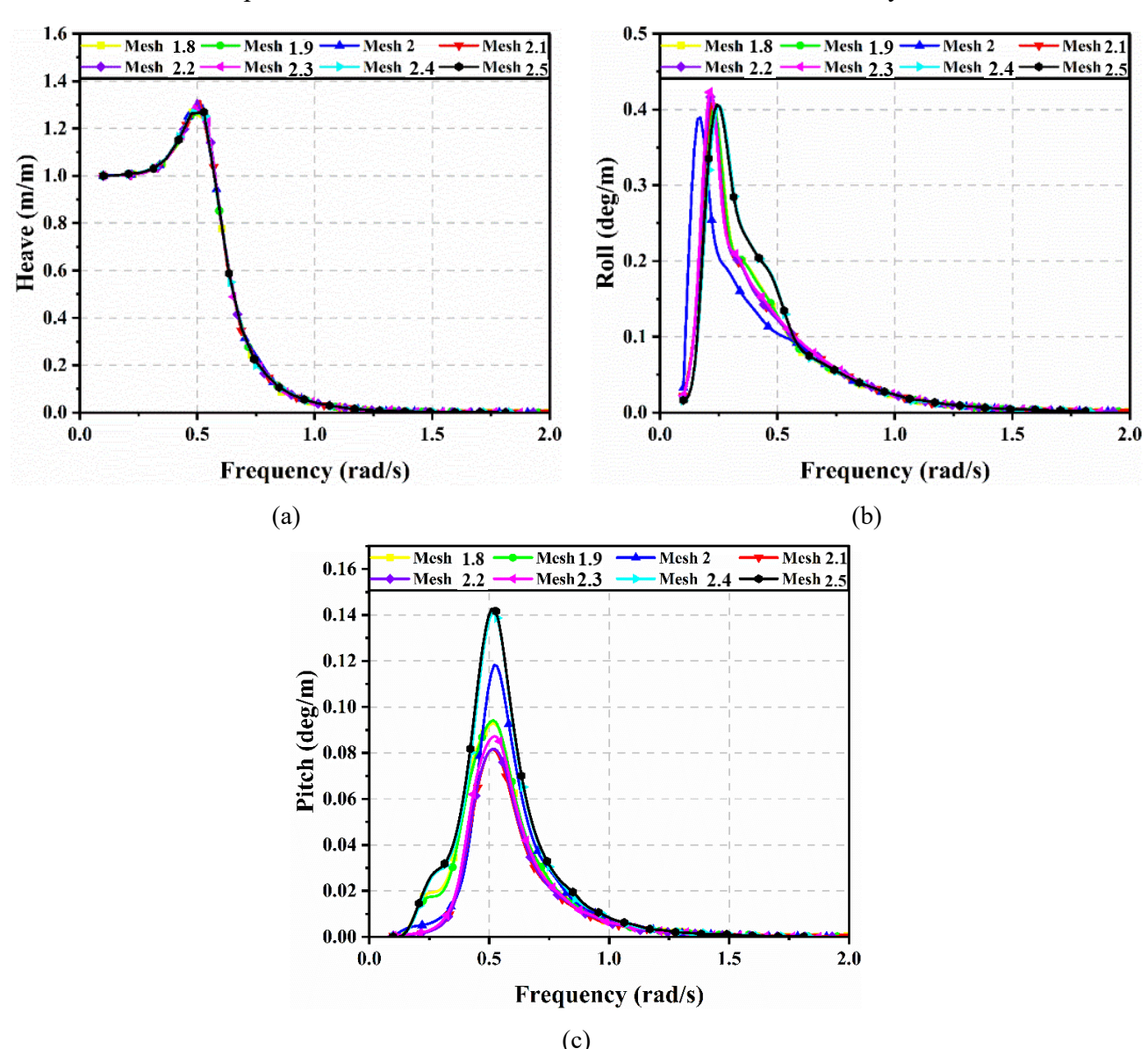


Figure 6. Response amplitude operator of floating structure in: (a) Heave, (b) Roll, and (c) Pitch

3.3 Motion response

The results of the time-domain analysis of the structure's motion response, considering environmental conditions in the form of irregular waves and currents, are presented in Figure 7. The study was conducted on the translational motion of the structure in the sway and heave directions. The results presented are statistical data, including the maximum value, mean, and standard deviation obtained from the simulation results for a 3600-second period for each mesh size variation. The sway motion demonstrates a maximum value of up to 84 m, an average of 48 m, and a standard deviation of 18 m, except for the 2.5 m mesh, which exhibits a substantial decrease. This finding suggests that employing a mesh with a coarser resolution is inadequate for accurately representing the wave-structure interaction. The heave motion exhibited a stable trend at mesh 1.8-2.4 m, with a maximum of 0.415 m, a mean of 0.115 m, and a standard deviation of 0.18 m.

The 2.5 m mesh once again demonstrated a significant decrease, suggesting a decline in the quality of the hydrodynamic force calculation. Furthermore, the rotational motion response of the structure, which consists of roll and pitch motion, is shown in Figure 8. The results of roll motion show relative stability in most meshes, except for those at 2.0 m and 2.5 m, which demonstrate substantial variations. The maximum value ranges from 0.34 to 0.36 deg, the mean is 0.075 deg, and the standard deviation is 0.09 deg, indicating the stability of the system. The pitch motion exhibits anomalous behavior on the 2.5 m mesh, with a maximum spike reaching 0.325 deg and a standard deviation of 0.95 deg. This suggests that the pressure distribution may be inaccurate due to the coarse panel discretization. The remaining meshes exhibit a maximum pitch response of approximately 0.03 deg, accompanied by negligible variations.

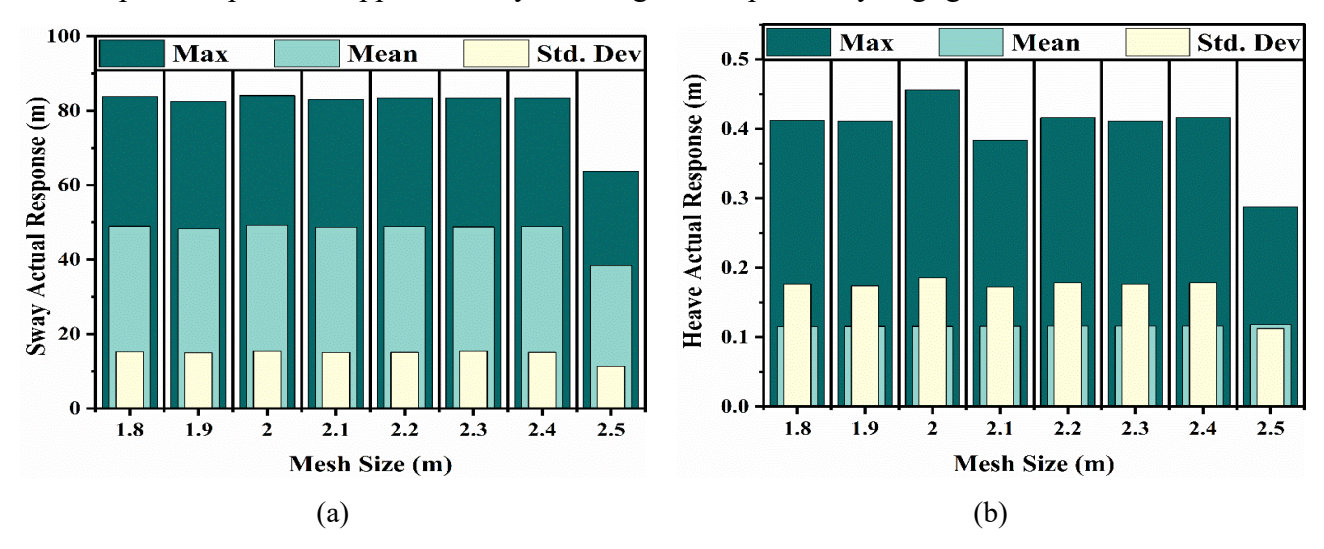


Figure 7. Translational actual motion statistics in: (a) Sway and (b) Heave

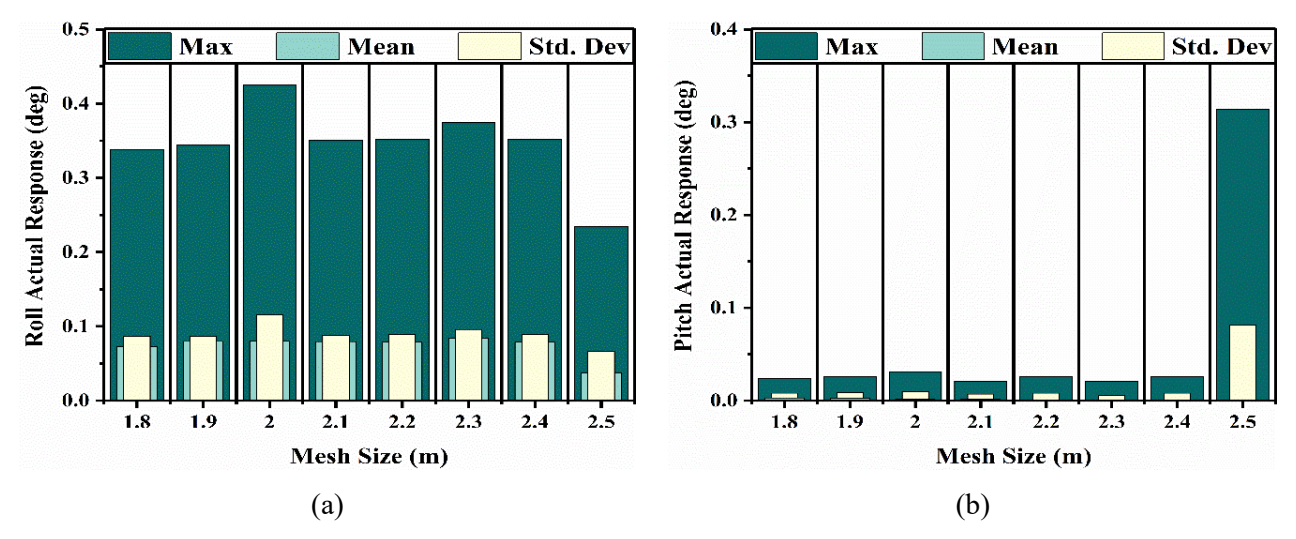


Figure 8. Rotation actual motion statistics in: (a) Roll and (b) Pitch

3.4 Mooring tension

Tension analysis of mooring systems is conducted to evaluate the capacity of the mooring line to withstand the dynamic loads of floating structures during operational conditions. It is essential to note that tension exceeding the maximum expected tension has the potential to induce failure in mooring systems, thereby resulting in structural instability. In this study, a spread mooring configuration was utilized, involving the attachment of four mooring lines to distinct sides of the structure. The mooring tension results are displayed in Figure 9, which presents the maximum, average, and standard deviation values over a simulation time of 3600 seconds. Mooring Line 1 exhibited the highest tension levels, with a maximum value of 5.4 MN, which remained relatively consistent across the range of mesh sizes. However, a slight decrease in tension was observed for the 2.5 m mesh.

The average tension levels attained during the simulation were found to be close to the maximum value, with a low standard deviation. This finding suggests that the tension levels remained relatively stable at a high level throughout the simulation. Mooring Line 2 exhibited reduced and stable tension due to the 90° wave and current directions, which prompted the structure to shift towards Mooring 2, resulting in the slackening of the rope. The maximum tension on Line 2 was 4.75 MN, with an average of 4.45 MN. Mooring Line 3, which is oriented parallel to Line 2, exhibits a comparable trend. However, at a mesh size of 2.5 m, there is an increase in tension due to an inaccurate representation of the fluid-structure interaction, resulting from the mesh size being too coarse.

Mooring Line 4 exhibited a similar pattern to Line 1, demonstrating a shift from the mooring with a maximum tension of 5.45 MN, an average of 5.2 MN, and a low deviation, suggesting stable load conditions. A general analysis indicates that the discrepancy in mesh size has a negligible impact on the outcomes of mooring tension assessments. This discrepancy can be attributed to the utilization of the Morison equation approach in the simulation, wherein the mooring system is discretized into nodes per unit length. This approach has been demonstrated to facilitate the representation of geometry with high resolution while maintaining accuracy in capturing the drag force, even when employing different mesh variations on the main structure.

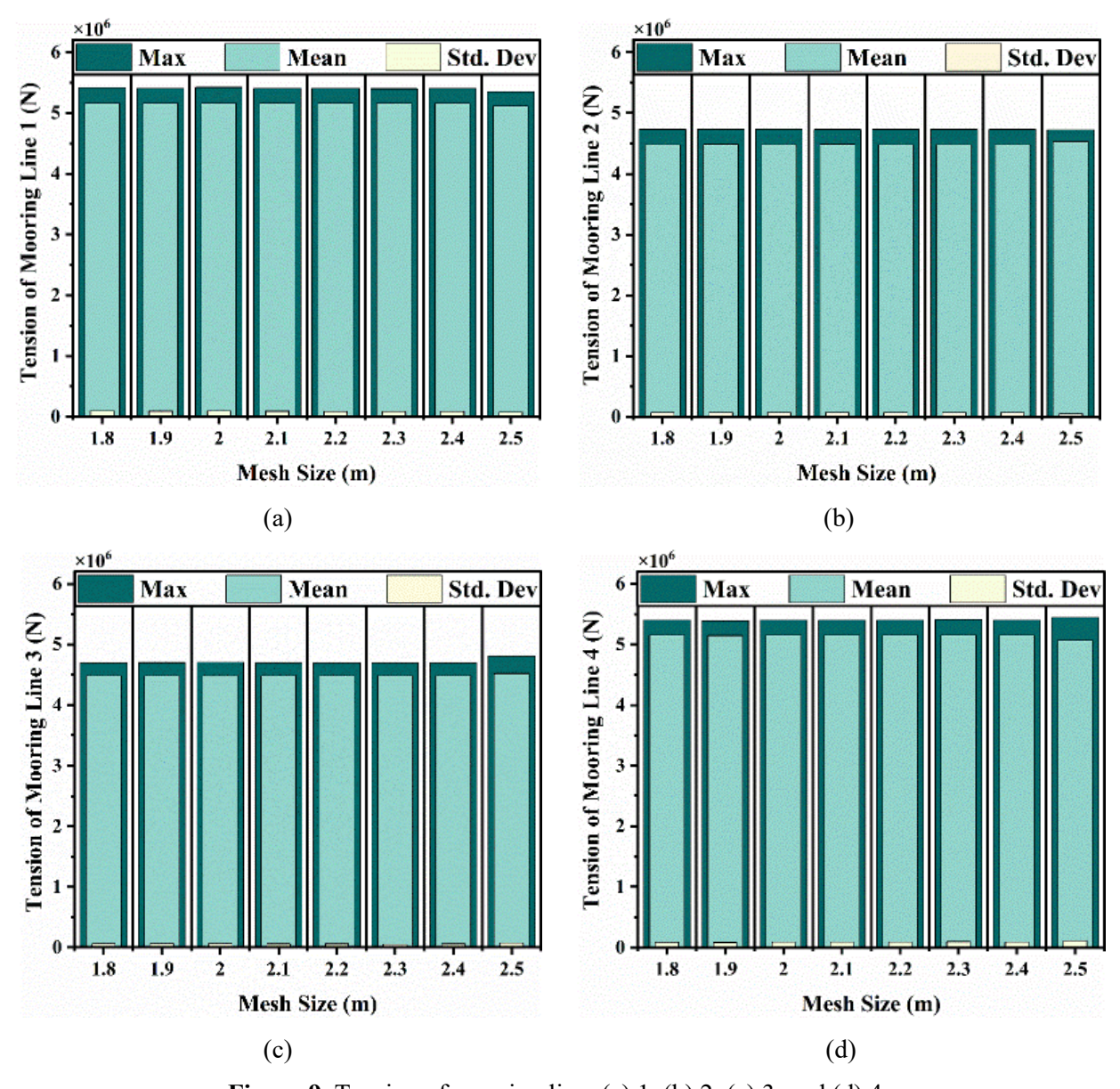


Figure 9. Tension of mooring line: (a) 1, (b) 2, (c) 3, and (d) 4

4 Conclusions

This study investigated the hydrodynamic performance and stability of a floating structure integrated with a 500 m CWP and mooring system, simulated at full scale using ANSYS AQWA. The results showed that the mesh size had a significant effect on the stability response prediction. Mesh sizes of 1.8, 2.1, 2.2, and 2.3 m produced stable responses, while sizes of 1.9, 2.0, 2.4, and 2.5 m showed inconsistent results. Specifically, a net size of 2.5 m resulted in deviations of up to 33% in surge, heave, and roll movements, with pitch being the most sensitive parameter. This indicates that the correlation between net size and stability results is not always linear. In terms of global stability, the integration of a 500 m CWP increased the hydrodynamic load but did not cause significant disruption to the overall stability of the floating structure. The mooring system was also proven effective, with relatively consistent tension responses despite variations in mesh size, thereby maintaining structural stability under irregular wave and current conditions. These findings confirm that proper mesh discretization is a key factor in ensuring reliable hydrodynamic predictions. At the same time, the mooring system plays a crucial role in maintaining the stable performance of the floating structure integrated with CWP.

References

- 1. T. Z. Ang, M. Salem, M. Kamarol, H. S. Das, M. A. Nazari, and N. Prabaharan, "A comprehensive study of renewable energy sources: Classifications, challenges and suggestions," *Energy Strateg. Rev.*, vol. 43, article no. 100939, 2022.
- 2. E. L. Vine, "Breaking down the silos: The integration of energy efficiency, renewable energy, demand response and climate change," *Energy Effic.*, vol. 1, no. 1, pp. 49-63, 2008.
- 3. K. Kartheekeyan, A. Baig, and N. R. Mahanta, "Exploring the potential of floating architecture & its energy challenges in the UAE," *Renew. Energy Electr. Technol.*, vol. 559, article no. 03012, 2024.
- 4. E. Begovic and S. Mancini, "Stability and seakeeping of marine vessels," *J. Mar. Sci. Eng.*, vol. 9, no. 2, article no. 222, 2021.
- 5. R. Hisamatsu and T. Utsunomiya, "A study on coupled behavior analysis and position keeping system for OTEC plantship and cold water pipe," *J. Japan Soc. Nav. Archit. Ocean Eng.*, vol. 32, pp. 193-207, 2021.
- 6. G. Pang, C. Wan, L. Sui, S. Zhu, H. Liu, G. Li, T. Yuan, Y. Hu, Q. Tao, and X. Huang, "Dynamic response simulation for a novel single-point mooring gravity-type deep-water net cage under irregular wave and current," *Appl. Sci.*, vol. 15, no.3, article no. 1570, 2025.
- 7. B. R. Reguram, S. Surendran, and S. K. Lee, "Application of fin system to reduce pitch motion," *Int. J. Nav. Archit. Ocean Eng.*, vol. 8, no. 4, pp. 409-421, 2016.
- 8. M. I. Habib, R. Adiputra, A. R. Prabowo, E. Erwandi, N. Muhayat, T. Yasunaga, S. Ehlers, and M. Braun, "Internal flow effects in OTEC cold water pipe: Finite element modelling in frequency and time domain approaches," *Ocean Eng.*, vol. 288, article no. 116056, 2023.
- 9. Y. M. Lutfi, R. Adiputra, A. R. Prabowo, T. Utsunomiya, E. Erwandi, and N. Muhayat, "Assessment of the stiffened panel performance in the OTEC seawater tank design: Parametric study and sensitivity analysis," *Theor. Appl. Mech. Lett.*, vol. 13, no.4, article no. 100452, 2023.
- 10. Rasgianti, R. Adiputra, A. D. Nugraha, R. B. Sitanggang, W. W. Pandoe, T. Yasunaga, and M. A. Santosa, "System parameters sensitivity analysis of ocean thermal energy conversion," *Emerg. Sci. J.*, vol. 8, no. 2, pp. 428-448, 2024.
- 11. R. Rasgianti, R. Adiputra, A. D. Nugraha, N. Firdaus, R. B. Sitanggang, N. Puryantini, and T. Yusunaga, "Design optimization of stiffening system for ocean thermal energy conversion (OTEC) cold water pipe (CWP)," *Result Eng.*, vol. 23, article no. 102863, 2024.
- 12. H. A. Al Kautsar, R. Adiputra, B. Kusharjanta, A. R. Prabowo, and H. Carvalho, "Preliminary assessment of a novel OTEC CWP design using sand-filled sandwich pipe," *Innovative Eco-Mater. Green prod.*, vol. 632, article no. 03006, 2025.
- 13. P. S. Asmara, Sumardiono, B. D. Alfanda, K. Abdullah, and A. N. Rochmad, "Study of offshore patrol vessel models for seakeeping and maneuvering improvement using anti-rolling fins," *Earth Environ. Sci.*, vol. 972, article no. 012012, 2022.
- 14. Y. Wang and Z. Ti, "Numerical modeling of hydrodynamic added mass and added damping for elastic bridge pier," *Adv. Bridg. Eng.*, vol. 4, article no. 24, 2023.

- 15. R. Adiputra, M. I. Firdaus, and N. Firdaus, "Coupled motion analysis of a ship-shaped floater and the coldwater pipe for OTEC implementation," *in the ASME 2024 43rd International Conference on Ocean, Offshore and Arctic Engineering*, Singapore, Singapore, 2024.
- 16. R. Hisamatsu and T. Utsunomiya, "Coupled response characteristics of cold water pipe and moored ship for floating OTEC plant," *Appl. Ocean Res.*, vol. 123, article no. 103151, 2022.
- 17. A. J. Hermans, "A boundary element method for the interaction of free-surface waves with a very large floating flexible platform," *J. Fluids Struct.*, vol. 14, no. 7, pp. 943-956, 2000.
- 18. A. Widyatmoko, S. Samuel, P. Manik, and A. Trimulyono, "Analysis of the effect of bilge keel length on rolling motion in a 14 m patrol boat," *Warta Penelitian Perhubungan*, vol. 33, no. 1, pp. 1-10, 2021. (*in Indonesian*).
- 19. R. Adiputra, F. N. Fauzi, N. Firdaus, E. M. Suyanto, A. Kasharjanto, N. Puryantini, E. Erwandi, R. Rasgianti, and A. R. Prabowo, "Roundness and slenderness effects on the dynamic characteristics of spar-type floating offshore wind turbine," *Curved Layer. Struct.*, vol. 10, no. 1, article no. 20220213, 2023.
- 20. L. Papillon, R. Costello, and J. V. Ringwood, "Boundary element and integral methods in potential flow theory: A review with a focus on wave energy applications," *J. Ocean Eng. Mar. Energy*, vol. 6, no. 3, pp. 303-337, 2020.
- 21. R. Adiputra, M. I. Firdaus, N. Firdaus, A. R. Prabowo, G. G. Salamena, and A. M. Faizatama, "Hydrodynamic responses of OTEC floating platform in operating and dismantling states," *in the 15th International Conference on Renewable and Clean Energy (ICRCE 2025)*, Fukuoka, Japan, 2025.
- 22. K. T. Ma, Y. Luo, T. Kwan, and Y. Wu, *Mooring System Engineering for Offshore Structures*, Texas: Gulf Professional Publishing, 2019.
- 23. Y. J. Kwon, B. W. Nam, N. Kim, D. H. Jung, S. Y. Hong, and H. J. Kim, "Numerical and experimental study on motion response of 1MW OTEC platform," *J. Ocean Eng. Technol.*, vol. 31, no. 2, pp. 81-90, 2017.
- 24. I. Zabala, J. C. C. Henriques, T. E. Kelly, P. P. Ricci, and J. M. Blanco, "Post-processing techniques to improve the results of hydrodynamic boundary element method solvers," *Ocean Eng.*, vol. 295, article no. 116913, 2024.
- 25. W. Shin, K. J. Paik, Y. H. Jang, M. J. Eom, and S. Lee, "A numerical investigation on the nominal wake of KVLCC2 model ship in regular head waves," *Int. J. Nav. Archit. Ocean Eng.*, vol. 12, pp. 270-282, 2020.